Fish and Shellfish Immunology 84 (2019) 787–794

Contents lists available at ScienceDirect

Fish and Shellfish Immunology

journal homepage: www.elsevier.com/locate/fsi

Full length article

Molecular characterization of a new fish specific chemokine CXCL_F6 in large yellow croaker (*Larimichthys crocea*) and its role in inflammatory response

Yinnan Mu[a], Shimin Zhou[a], Ning Ding[a], Jingqun Ao[c], Xinhua Chen[a,b,*]

[a] Institute of Oceanology, College of Animal Sciences, Fujian Agriculture and Forestry University, Fuzhou, 350002, China
[b] Laboratory for Marine Biology and Biotechnology, Qingdao National Laboratory for Marine Science and Technology, Qingdao, China
[c] Key Laboratory of Marine Biogenetic Resources, Third Institute of Oceanography, State Oceanic Administration, Xiamen, 361005, China

ARTICLE INFO

Keywords:
CXC chemokine
CXCL_F6
Chemotaxis
Large yellow croaker (*Larimichthys crocea*)
Inflammatory response

ABSTRACT

Chemokines are a superfamily of structurally related chemotactic cytokines exerting significant roles in regulating cell migration and activation. Currently, five subgroups of fish specific CXC chemokines, named CXCL_F1-CXCL_F5, have been identified in teleost fish. However, understanding of the functions of these fish specific CXC chemokines is still limited. Here, a new member of fish specific CXC chemokines, *Lc*CXCL_F6, was cloned from large yellow croaker *Larimichthys crocea*. Its open reading frame (ORF) is 369 nucleotides long, encoding a peptide of 122 amino acids (aa). The deduced *Lc*CXCL_F6 protein contains a 19-aa signal peptide and a 103-aa mature polypeptide, which has four conserved cysteine residues (C^{28}, C^{30}, C^{56}, and C^{72}), as found in other known CXC chemokines. Phylogenetic analysis showed *Lc*CXCL_F6 formed a separate clade with sequences from other fish species, tentatively named CXCL_F6, distinct from the clades formed by fish CXCL_F1-5 and mammalian CXC chemokines. The *Lc*CXCL_F6 transcripts were constitutively expressed in all examined tissues and significantly up-regulated in the spleen and head kidney tissues by poly (I:C) and *Vibrio alginolyticus*. Its transcripts were also detected in primary head kidney leukocytes (HKLs), peripheral blood leucocytes (PBLs), and large yellow croaker head kidney (LYCK) cell line, and significantly up-regulated by poly(I:C), lipopolysaccharide (LPS), and peptidoglycan (PGN) in HKLs. Recombinant *Lc*CXCL_F6 protein (r*Lc*CXCL_F6) could not only chemotactically attract monocytes/macrophages and lymphocytes from PBLs, but also enhance NO release and expression of proinflammatory cytokines (TNF-α, IL-1β, and CXCL8) in monocytes/macrophages. These results indicate that *Lc*CXCL_F6 plays a role in mediating the inflammatory response.

1. Introduction

The chemokines, a large family of small, secreted proteins, are best known for their ability to stimulate the migration and localization of cells, most notably leukocytes, through cell surface G protein-coupled hepta-helical receptors [1]. In addition, chemokines also play important roles in diverse immunological and physiological processes, such as activation of T lymphocytes and macrophages, angiogenesis, organogenesis, and neurological development [2,3]. Chemokine monomer consists of a central three stranded β-sheets, an overlying C-terminal α-helix, and a short unstructured N-terminus that plays a critical role in receptor activation [4]. The primary characteristic of chemokines is the four structurally important cysteine residues within the mature protein, which maintain the structure of the chemokine monomer by forming disulfide bonds [5]. Variation in the precise configuration of the two N-terminal cysteines allows chemokines to be split into four major subfamilies, including CC, CXC, CX3C, and CX [6,7].

In mammals, the CXC chemokines are known to function in chemotaxis of neutrophils, monocytes and lymphocytes [8–10]. The mammalian CXC subfamily consists of 17 members, but each species has slightly variable numbers of genes, with 16 members for human (lacking CXCL15), 15 for mouse (lacking CXCL6 and CXCL8) and a smaller number identified from other mammalian species [10]. CXC chemokines are further classified into ELR-positive or ELR-negative groups based on the presence of a conserved ELR (glutamic acid-leucine-arginine) motif [11]. The ELR-positive group contains CXCL1-3, CXCL5-8, and CXCL15, while ELR-negative group includes CXCL4, CXCL9-14, and CXCL16-17 [6,12].

Currently, an increasing number of CXC chemokines have been identified in teleost fish, for instance, 23 CXC chemokines have been

* Corresponding author. No.15 Shangxiadian Road, Cangshan District, Fuzhou, 350002, Fujian, China.
E-mail address: chenxinhua@tio.org.cn (X. Chen).

https://doi.org/10.1016/j.fsi.2018.10.068
Received 24 July 2018; Received in revised form 13 September 2018; Accepted 25 October 2018
Available online 26 October 2018
1050-4648/

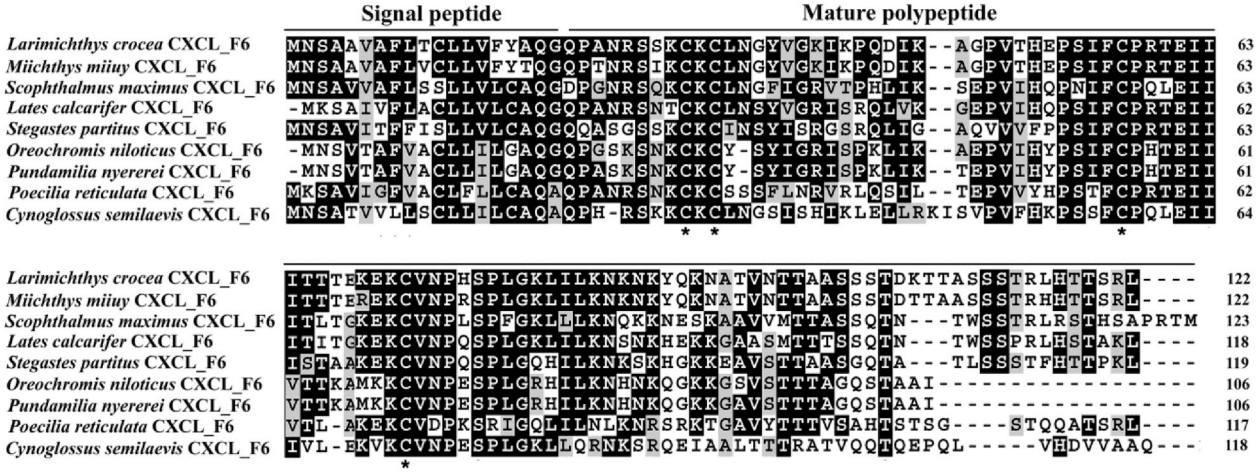

Fig. 1. Alignment of the CXCL_F6 amino acid sequences from large yellow croaker and other fish.
The four conserved cysteine residues are shown with asterisks. The identical residues are shaded in black. The NCBI accession numbers for the CXCL_F6 protein sequences are listed in Supplementary Table 2.

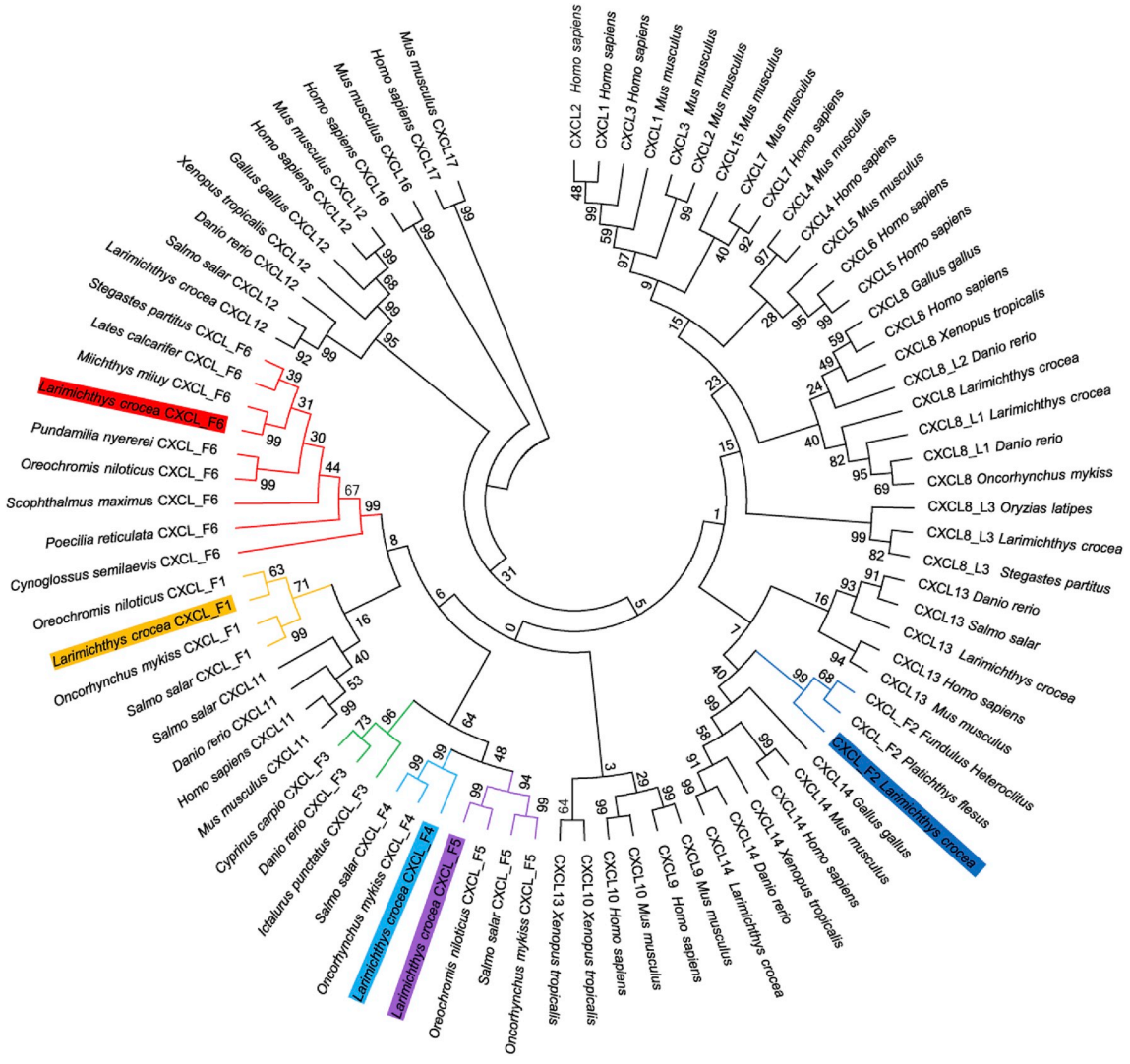

Fig. 2. Phylogenetic tree of CXC chemokines.
A phylogenetic tree was constructed based on the amino acid sequences of CXC chemokines by MEGA 6.06 using neighbour-joining method. The numbers on nodes represent frequency per 100 bootstrap replications in a total of 10000. The NCBI accession numbers for CXC chemokine protein sequences used here are listed in Supplementary Table 2.

identified in zebrafish [10,13], 17 in channel catfish (*Ictalurus punctatus*) [10], 11 in brown trout (*Salmo trutta*) [7], and more than 10 in rainbow trout (*Oncorhynchus mykiss*) [14]. However, CXCL1-7, CXCL9-10, and CXCL15-17 homologues have not been found in any fish species yet. Correspondingly, a number of fish specific CXC chemokines (CXCL_F) have been discovered in various fish species, which are phylogenetically divided into five subgroups, CXCL_F1-CXCL_F5 [7]. The first fish specific CXC chemokine CXCL_F1 (CXCd) was reported in rainbow trout and its expression significantly increased in spleen following bacterial challenge or vaccination [14,15]. In brown trout, the mRNA transcription of CXCL_F1, CXCL_F2, CXCL_F4, and CXCL_F5 increased in spleen and head kidney under both viral haemorrhagic septicaemia virus and *Yersinia ruckeri* stimulation [7]. The expression levels of CXCL_F2 from large yellow croaker was significantly up-regulated after stimulation with bacterial vaccine and its recombinant protein obviously attracted monocytes, lymphocytes, and eosinophils [6]. CXCL18 and CXCL20, two fish specific CXC chemokines of channel catfish were also induced after *Edwardsiella ictaluri* and *Flavobacterium columnare* infections [10].

The large yellow croaker (*Larimichthys crocea*) is one of the most economically important marine fish in China and East Asia [16]. So far, six CXC chemokines, including CXCL12 [17], CXCL13 [18], three CXCL8 [19–21], and CXCL_F2 [6], have been identified in this species. In this study, we identified and characterized a new member of fish specific chemokines from large yellow croaker (*Lc*CXCL_F6). We found that *Lc*CXCL_F6 was constitutively expressed in all tissues examined and was significantly up-regulated in the spleen and head kidney tissues by poly (I:C) and *Vibrio alginolyticus*. The *Lc*CXCL_F6 expression was also detected in three immune-related cells and increased in HKLs by poly (I:C), LPS, and PGN. Additionally, recombinant *Lc*CXCL_F6 protein (r*Lc*CXCL_F6) not only exhibited chemotactic activity for monocytes/macrophages and lymphocytes from PBLs, but also enhanced the NO release and up-regulated the expression of pro-inflammatory cytokines in monocytes/macrophages from head kidney.

2. Materials and methods

2.1. Fish and challenge experiments

Large yellow croakers (mean mass: 104 ± 13.6 g; mean length: 21 ± 1.5 cm) were purchased from a mari-culture farm at Ningde, Fujian, China. Fish were cultivated in flow-through seawater at 16 °C. After 7 days of acclimation, large yellow croakers were divided into three groups of 30 fish each. The two experimental groups were intraperitoneally injected with poly(I:C) (Sigma-Aldrich, USA; 1 mg/mL in PBS) or *Vibrio alginolyticus* (1.0×10^8 CFU/mL) at a dose of 0.2 mL/100 g fish. The control group of 30 fish was injected with sterilized PBS (pH 7.4) at a dose of 0.2 mL/100 g fish. Spleen and head kidney tissues from six fish of each group were collected at different time points (6, 12, 24, 48 and 72 h) after injection, frozen immediately in liquid nitrogen, and stored at −80 °C for next use.

2.2. Primary cells

Primary peripheral blood leukocytes (PBLs) were isolated as previously described [21]. Briefly, the blood was sampled from the caudal vein sinus of large yellow croaker, diluted by Leibovitz's medium (L-15 medium; Gibco, USA), loaded onto freshly prepared 34%/51% Percoll (GE, USA) density gradients and separated via centrifugation at 650 × *g* for 30 min at 4 °C. PBLs were then taken from the interface between 34%/51% Percoll and diluted to a final concentration of 1×10^6 cells/mL in L-15 medium.

Primary head kidney monocytes/macrophages (PKMs) were isolated according to the procedure described previously [22]. Briefly, head kidney tissue was collected and pushed gently through 70 μm stainless steel screens. The resultant cell suspension was loaded onto 34%/51% Percoll density gradients, followed by centrifugation at 650*g* for 30 min at 4 °C. Primary head kidney leukocytes (HKLs) were collected from the gradient interface and put on culture dish for 2 h at 28 °C until cell attachment. After removing nonadherent cells by two washes with L-15 medium, attached cells were digested with trypsin (Gibco, USA). The resulting cell suspension was centrifuged at 1500 rpm for 10 min to remove the trypsin, and PKMs were then collected and diluted to a final concentration of 1×10^6 cells/mL in L-15 medium.

Large yellow croaker head kidney (LYCK) cell line was established and maintained in our laboratory [23].

2.3. Cloning and sequence analysis of LcCXCL_F6 cDNA

The *Lc*CXCL_F6 gene sequence was predicted from the genome database of large yellow croaker (JRPU00000000) [16]. To obtain the open reading frame (ORF) of *Lc*CXCL_F6, primer set of *Lc*CXCL_F6−F1 and -R1 was designed according to the predicted *Lc*CXCL_F6 sequence (Supplementary Table 1). Using first strand cDNA from total RNA of large yellow croaker spleen as a template, PCR was performed using EasyPfu DNA Polymerase (TransGen Biotech, China) under the following conditions: 95 °C for 1 min, then 35 cycles of 95 °C for 30 s, 57 °C for 30 s, 72 °C for 1 min, followed by a final extension at 72 °C for 10 min. The resulted PCR product was inserted into pMD20-T simple vector (Takara, China) and sequenced. Multiple alignments were performed using the CLUSTAL Omega program (https://www.ebi.ac.uk/Tools/msa/clustalo/). Protein domains were predicted by Simple Modular Architecture Research Tool (SMART) [24]. Signal peptide was predicted by using SignalP 4.1 [25]. Phylogenetic tree was constructed with Molecular Evolution Genetics Analysis (MEGA) software version 6.06 using the neighbour-joining method [26]. The NCBI accession numbers for CXC chemokine protein sequences used here are listed in Supplementary Table 2.

2.4. Expression analysis of LcCXCL_F6 by real-time PCR

Various tissues including blood, brain, gills, head kidney, heart, intestine, liver, muscle, skin, and spleen were collected from five large yellow croakers. Total RNA was isolated from a pooled tissue of five fish and reverse-transcribed into first strand cDNA. Real-time PCR was performed with the primer set of *Lc*CXCL_F6−F3 and -R3 (Supplementary Table 1). The β-actin gene was amplified with the primer set of Actin-F1 and -R1 as internal control (Supplementary Table 1). PCR cycles were performed on the Mastercycler epgradient realplex 4 system (Eppendorf, Germany) with SYBR Premix Ex Taq™ kit (Takara, China). The cycling conditions were 1 min at 95 °C, followed by 40 cycles of 95 °C for 5 s, 58 °C for 15 s, and 72 °C for 20 s. The relative expression of *Lc*CXCL_F6 gene was normalized against β-actin using the $2^{-\Delta\Delta CT}$ method [20], and was expressed relative to *Lc*CXCL_F6 expression in the brain.

To further understand the modulation of *Lc*CXCL_F6 gene expression, total RNA was extracted from spleen and head kidney tissues of six fish collected at each time point (12, 24, 48 and 72 h) post-induction with poly (I:C) or *V. alginolyticus*, respectively. Real-time PCR was performed using the conditions described above. The relative expression levels of *Lc*CXCL_F6 gene were normalized by β-actin. Fold change of *Lc*CXCL_F6 gene expression levels was expressed as the ratio of the normalized gene expression levels in fish injected with poly (I:C) or *V. alginolyticus* versus those in fish injected with PBS at the same time point. The data obtained from three independent assays with three replicates in each assay were subjected to statistical analysis.

To analyze the expression of *Lc*CXCL_F6 gene in three immune-related cells, total RNA was extracted from 1×10^6 of HKLs, PBLs, and LYCK cells using the ReliaPrep RNA Cell Miniprep System (Promega, USA), respectively. Real-time PCR was performed as described above. The expression levels of *Lc*CXCL_F6 were calculated by normalization to

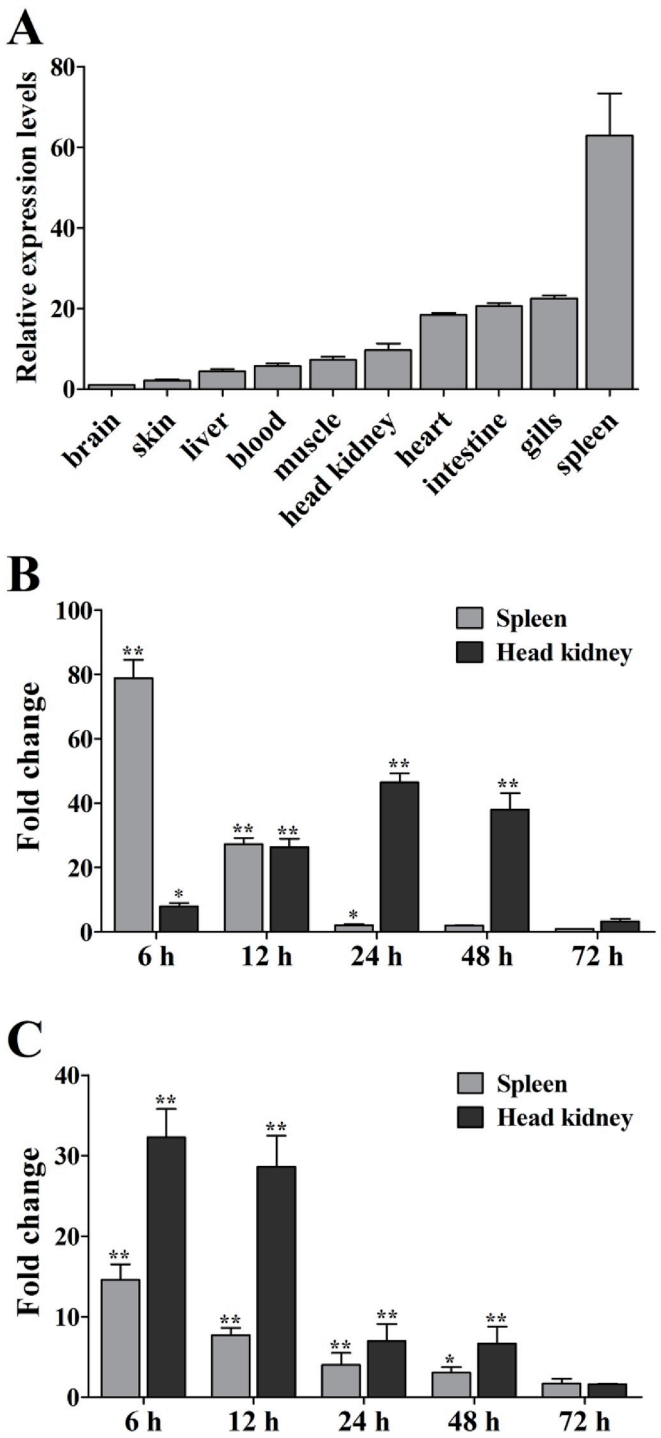

Fig. 3. Tissue expression analysis of *Lc*CXCL_F6 gene.

(A) Relative expression of *Lc*CXCL_F6 transcripts in different tissues of large yellow croaker (five fish), including blood, brain, gills, head kidney, heart, intestine, liver, muscle, skin, and spleen. Modulation of *Lc*CXCL_F6 gene expression in spleen and head kidney based on induction with poly (I:C) (B) and *Vibrio alginolyticus* (C). Spleen and head kidney tissues were collected from six fish at each time point (6, 12, 24, 48, and 72 h) after induction. The β-actin expression was used as an internal control for real-time PCR. Deviation bars represent the standard error of the mean (SEM) of three independent PCR assays with three replicates in each assay. Statistically significant differences were indicated with asterisks where $^{*}p < 0.05$ and $^{**}p < 0.01$.

β-actin using the $2^{-\triangle\triangle CT}$ method and expressed as the ratio of the *Lc*CXCL_F6 expression level in LYCK cells.

HKLs were further treated with a final concentration of 40 μg/mL poly(I:C), 50 μg/mL LPS (Sigma Aldrich), or 20 μg/mL PGN for 6, 12, and 24 h. Total RNA was extracted from these cells for real-time PCR analysis of *Lc*CXCL_F6 expression. The relative expression levels of *Lc*CXCL_F6 were normalized by β-actin and expressed as fold changes by comparing the normalized gene expression levels in cells treated with poly(I:C), LPS, or PGN with those in the PBS-treated cells at the corresponding time point.

2.5. Expression and purification of recombinant LcCXCL_F6

*Lc*CXCL_F6 gene fragment excluding the signal peptide was amplified with the primer set of *Lc*CXCL_F6−F2 and -R2 (Supplementary Table 1) and inserted into pET-His vector. The constructed recombinant plasmid pET-*Lc*CXCL_F6 was transformed into *E. coli* Rosetta competent cells. Expression of r*Lc*CXCL_F6 was induced by 0.1 mM isopropyl-β-D-1-thiogalactopyranoside (IPTG) at 37 °C for 4 h, and was analyzed by SDS-PAGE. The r*Lc*CXCL_F6 was purified by Ni-NTA rilotriacetic acid (NI-NTA) affinity chromatography under nondenaturing condition using ProBond™ Purification System (Invitrogen, USA). The resulting r*Lc*CXCL_F6 was then dialyzed against PBS, filtered with a sterile 0.2 μm filter, and stored at −80 °C. Recombinant GST protein (rGST) was expressed and purified in the same system as a control.

2.6. Chemotaxis assay in vitro

In vitro chemotaxis assay was performed using a 24-well Costar Transwell apparatus (Corning, USA) as described previously [6]. Purified r*Lc*CXCL_F6 was diluted to 1, 10, 30, 50 μg/mL in L-15 medium. Then, 600 μL of each diluted protein solution was added to lower chamber of the transwell unit. Polycarbonate filters with a pore diameter of 3 μm were then placed onto the lower wells, and 100 μL of PBLs (1×10^5 cells) were added in the upper chamber. The unit was incubated at 22 °C for 4 h. At the end of reaction, cells migrated to the lower chamber and the reverse side of polycarbonate filters (digested by trypsin) were counted. Finally, the migrated cells were collected for morphological identification using rapid Wright-Giemsa staining (NJJCTECH, China). Each experiment was repeated three times. Purified rGST (10 μg/mL) was used as control in the chemotaxis assay.

2.7. Nitric oxide assays

PKMswere cultured in 96-well plates (3×10^5 cells/well) and treated with r*Lc*CXCL_F6 (at a final concentration of 0.01, 0.1, 1, and 5 μg/mL) or the same concentration of rGST (as a control). The cells were incubated at 28 °C for 72 h and the cell culture supernatants were collected for analyses of NO concentration. Absorbance values at 540 nm were acquired and nitrite concentration was determined using a sodium nitrite standard curve based on the Griess reaction with NO determination kit (Beyotime, China). All data were obtained from three independent experiments with three replicates in each experiment.

2.8. Expression analyses of iNOS and pro-inflammatory cytokine genes by real-time PCR

PKMs (3×10^6 cells/well) were cultured in 6-well plates at 28 °C for 2 h and treated with r*Lc*CXCL_F6 (at a final concentration of 10 ng/mL) or the same concentration of rGST (as a control). The cells were then harvested at 6, 12, and 24 h after treatment for expression analysis of iNOS and proinflammatory cytokine TNF-α, IL-1β, and CXCL8 genes. Real-time PCR was performed with the gene specific primers (Supplementary Table 1). The relative expression levels of each gene were normalized by β-actin and expressed as fold change by comparing the normalized gene expression levels in the r*Lc*CXCL_F6-treated cells

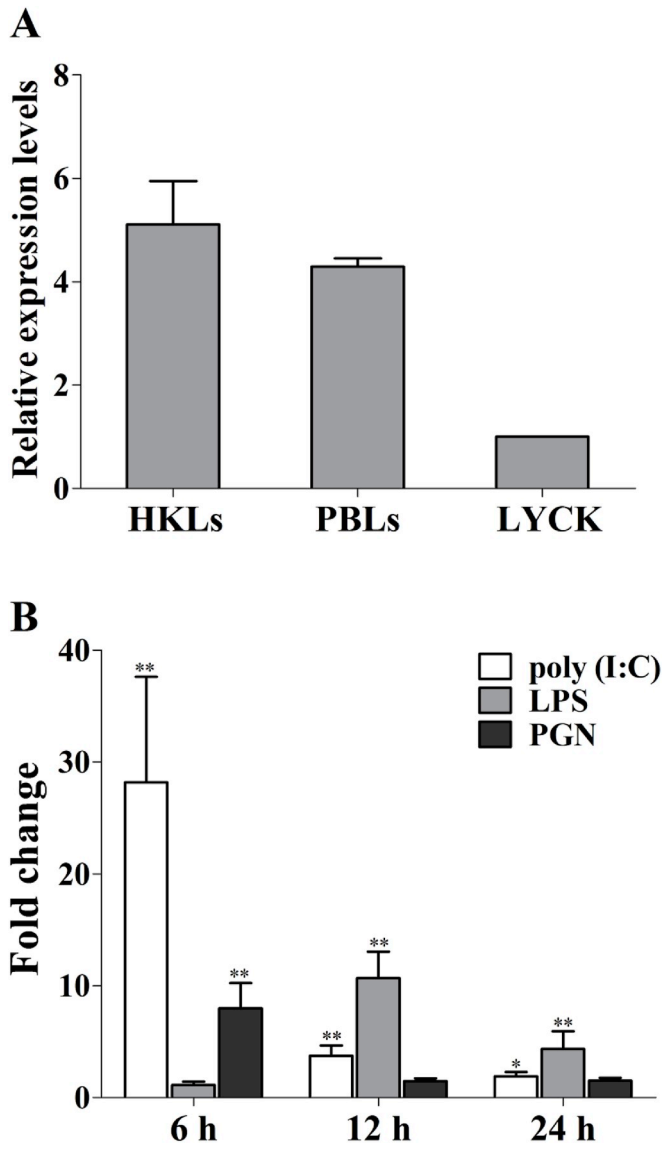

Fig. 4. *Lc*CXCL_F6 expression in immune-related cells.
(A) Relative expression levels of *Lc*CXCL_F6 gene were detected in head kidney leukocytes (HKLs), peripheral blood leucocytes (PBLs), and large yellow croaker head kidney (LYCK) cell line. (B) *Lc*CXCL_F6 expression analysis in HKLs stimulated with poly(I:C), LPS, or PGN. The HKLs were treated with PBS as a control. The relative expression levels of *Lc*CXCL_F6 were normalized by β-actin and expression as fold change compared with the control at each time point. Error bars represent SEM of three independent experiments. $^{*}p < 0.05$; $^{**}p < 0.01$.

with those in the rGST-treated cells at each time point. All data were obtained from three independent experiments with three replicates in each experiment.

2.9. Statistical analysis

All data were analyzed using GraphPad Prism 5 software and expressed as mean ± standard error of the mean (SEM) of three independent experiments. Student *t*-test was performed to check the statistical differences between the experimental and control groups. The $P < 0.05$ stands for statistically different and $P < 0.01$ for significantly different.

3. Results

3.1. Identification and characterization of LcCXCL_F6

The complete ORF of *Lc*CXCL_F6 gene was 369 nucleotides (nt) in length and encoded 122 amino acids (Supplementary Fig. 1). The first 19 amino acids were predicted to be the signal peptide. The deduced *Lc*CXCL_F6 protein contained four conserved cysteine residues (C^{28}, C^{30}, C^{56}, and C^{72}), as found in other CXC chemokines, and the first two cysteine residues were separated by a lysine (Fig. 1). *Lc*CXCL_F6 lacked the ELR motif. Phylogenetic analysis showed that most of the large yellow croaker CXC chemokines were clustered into known clades with their respective counterparts from other vertebrates with strong bootstrap support (Fig. 2). However, *Lc*CXCL_F6 formed a separate clade with sequences from other fish species, distinct from the clades formed by fish CXCL_F1-5 and mammalian CXC chemokines. Homology comparison showed that the *Lc*CXCL_F6 has a higher sequence identity of 48–93% with other fish CXCL_F6 proteins, but a relatively low identity with other subgroups of CXC chemokines (9–35%, Supplementary Table 2).

3.2. Tissue expression analysis of LcCXCL_F6 gene

Real-time PCR was used to investigate expression levels of *Lc*CXCL_F6 gene in various tissues. The results showed that the *Lc*CXCL_F6 transcripts could be detected in all tissues examined, with the highest levels in spleen and gills, and the lowest level in brain (Fig. 3A). Under stimulation with poly (I:C), *Lc*CXCL_F6 transcripts quickly increased in spleen with 79.0-fold increases at 6 h post-stimulation (Fig. 3B). However, in head kidney, the *Lc*CXCL_F6 expression reaching the peak was at 24 h post-stimulation with poly (I:C). Similarly, *Lc*CXCL_F6 transcriptional levels were significantly up-regulated in spleen and head kidney by *V. alginolyticus* and both reached the peak at 6 h post-stimulation, with 14.6- and 32.3-fold increases, respectively (Fig. 3C).

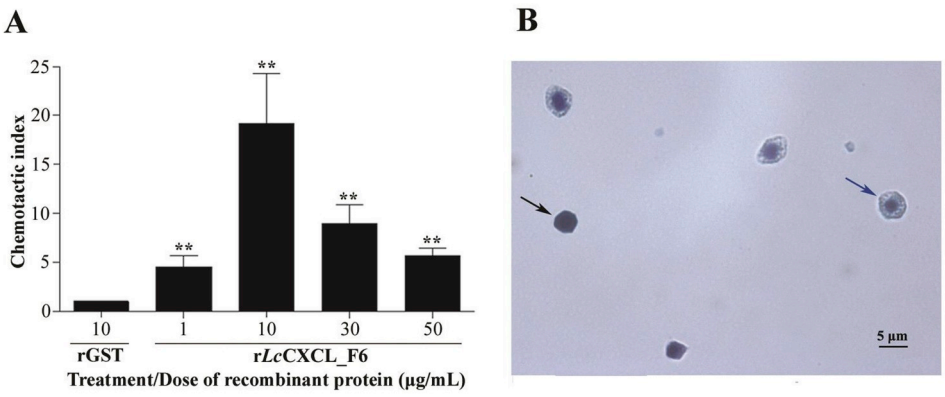

Fig. 5. Chemotactic activity of r*Lc*CXCL_F6.
(A) Chemotactic activity of r*Lc*CXCL_F6 to large yellow croaker PBLs at various concentrations. Recombinant GST was used as control. Deviation bars represent the standard error of the mean (SEM) of three independent experiments. Statistical differences are indicated with asterisks where $^{*}p < 0.05$ and $^{**}p < 0.01$. (B) Wright-Giemsa staining cell image (× 100). The attracted large yellow croaker peripheral blood cells were stained by Wright-Giemsa staining after chemotactic activity assay. Lymphocytes were pointed by black arrow and monocytes/macrophages by blue arrow. (For interpretation of the references to colour in this figure legend, the reader is referred to the Web version of this article.)

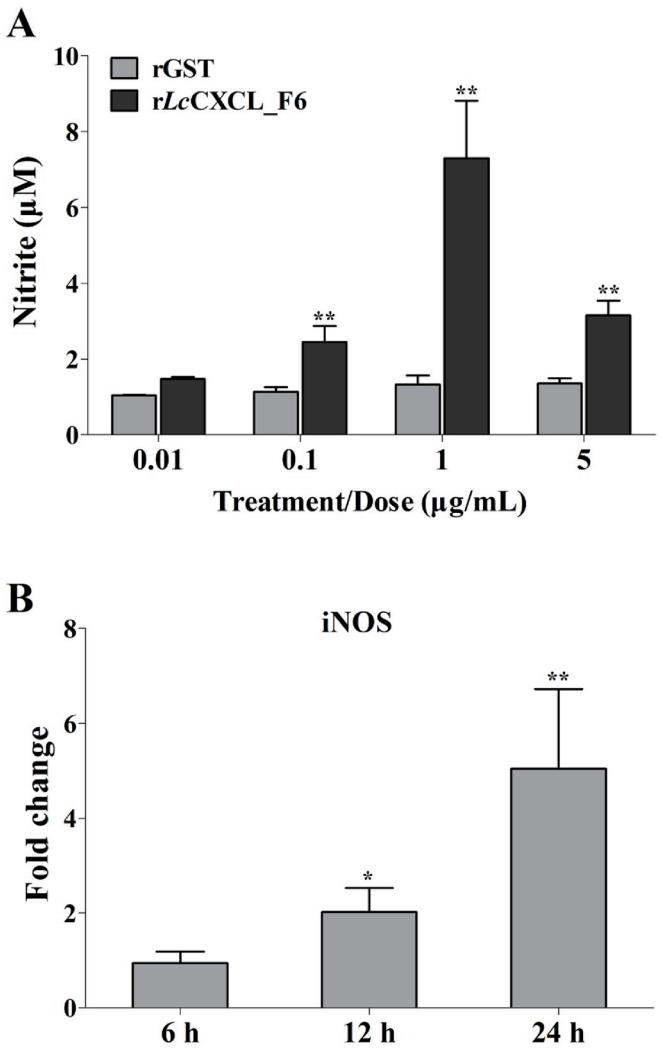

Fig. 6. Nitric oxide response and iNOS gene expression in PKMs treated with r*Lc*CXCL_F6.

(A) Nitric oxide production of primary head kidney macrophages (PKMs) treated with r*Lc*CXCL_F6. PKMs were treated with r*Lc*CXCL_F6 at final concentrations of 0.01, 0.1, 1 or 5 μg/mL, and the cell culture supernatants were harvested at 72 h after treatment. PKMs were treated with the same concentration of rGST as controls. Nitric oxide production was determined using the Griess reaction and nitrite concentration was calculated from the sodium nitrite standard curve based on the Griess reaction. (B) Expression analysis of iNOS gene in PKMs treated with r*Lc*CXCL_F6. PKMs were treated with r*Lc*CXCL_F6 at a final concentration of 1 μg/mL. PKMs were also treated with the same concentration of rGST as controls. The relative expression levels of iNOS were normalized by β-actin and expressed as fold change by comparing the normalized gene expression levels in the r*Lc*CXCL_F6-treated cells with those in the rGST-treated cells at each time point. All data were obtained from three independent experiments with three replicates in each experiment. Error bars represent SEM of three independent experiments. $^{*}p < 0.05$; $^{**}p < 0.01$.

3.3. Expression analysis of *LcCXCL_F6* in immune-related cells

As shown in Fig. 4A, *Lc*CXCL_F6 gene could be detected in HKLs, PBLs, and LYCK cells, and relatively high expression level was detected in HKLs. Furthermore, *Lc*CXCL_F6 expression levels were significantly up-regulated in HKLs by poly (I:C), LPS, and PGN, and reached the peaks at 6, 12, and 6 h post-stimulation, respectively (Fig. 4B).

3.4. Chemotaxis assays

To determine the chemotactic activity of *Lc*CXCL_F6, r*Lc*CXCL_F6 was produced in *E. coli* Rosetta and purified using immobilized Ni-NTA metal affinity chromatography (Supplementary Fig. 2). The purified r*Lc*CXCL_F6 showed obvious chemotactic activity to large yellow croaker PBLs at different concentrations of 1, 10, 30, and 50 μg/mL, and displayed the strongest ability to attract PBLs at 10 μg/mL (Fig. 5A). Comparatively, the control protein rGST had no chemotactic activity to PBLs. Then, the migrated cells were stained using Wright-Giemsa. It was found that the monocytes/macrophages and lymphocytes were main cell types attracted from PBLs (Fig. 5B).

3.5. Effect of *LcCXCL_F6* on iNOS gene expression and NO release

The r*Lc*CXCL_F6 could increase the NO production in the PKMs at a final concentration of 0.1, 1, and 5 μg/mL, and displayed the strongest ability at 1 μg/mL (Fig. 6A). Since NO is synthesized by iNOS in macrophages as a free radical [27], we then examined the effect of r*Lc*CXCL_F6 on iNOS gene expression. In the r*Lc*CXCL_F6-treated PKMs, the expression levels of iNOS gene were significantly up-regulated at 12 and 24 h, with 2- and 5-fold increases, respectively (Fig. 6B).

3.6. The rLcCXCL_F6 induced expression of pro-inflammatory cytokine genes in PKMs

To understand whether *Lc*CXCL_F6 could induce the expression of pro-inflammatory cytokine genes in monocytes/macrophages, we detected the expression levels of major pro-inflammatory cytokines TNF-α, IL-1β, and CXCL8 in the r*Lc*CXCL_F6-treated PKMs by real-time PCR. As shown in Fig. 7, the transcript levels of TNF-α, IL-1β, and CXCL8 were obviously up-regulated in the r*Lc*CXCL_F6-treated PKMs and had 164-, 5.6-, and 391-fold increases at 6, 12, and 12 h after treatment, respectively.

4. Discussion

Here, we identified a new member of fish specific CXC chemokines, *Lc*CXCL_F6, from large yellow croaker. As found in other known CXC chemokines, *Lc*CXCL_F6 also contains four conserved cysteine residues (Fig. 1), which are essential for the tertiary structure and classification of chemokines [28]. Currently, five subgroups of fish specific CXC chemokines, named CXCL_F1-CXCL_F5, have been identified in teleost fish [7]. Phylogenetic analysis based on the amino acid sequences of CXC chemokines from various organisms showed that *Lc*CXCL_F6 formed a separate clade with sequences from other fish species, distinct from the clades formed by fish CXCL_F1-5 and mammalian CXC chemokines (Fig. 2). *Lc*CXCL_F6 also has a relatively low sequence identity with the members from other CXC chemokine subgroups. Based on these data, *Lc*CXCL_F6 and its counterparts should be assigned to a new subgroup of fish specific CXC chemokines, tentatively named CXCL_F6.

The *Lc*CXCL_F6 transcripts were widely detected in various tissues, with the highest expression levels in spleen and gills, and the lowest level in brain (Fig. 3A), which are consistent with the tissue distribution of other CXCL_Fs. *Lc*CXCL_F2 mRNA was detected in various tissues, with the highest level in spleen [6]. Brown trout CXCL_F4 and CXCL_F5 were highly expressed in the spleen [7]. In rainbow trout, CXCL_F4 mRNA was highly transcribed in spleen, while CXCL_F5 transcripts were highly expressed in gills [14]. High expression of CXCL_Fs in fish spleen and gills suggests that the CXCL_Fs producing cells may be abundant at these two organs, which are two major immune-related organs in fish. Furthermore, similar to other CXCL_Fs [6,10,14,15], the transcription of *Lc*CXCL_F6 was significantly increased in spleen and head kidney under stimulation by poly (I:C) and *V. alginolyticus* (Fig. 3B and C), and increased in HKLs by poly(I:C), LPS and PGN (Fig. 4B). These results suggested that *Lc*CXCL_F6 may participate in immune responses against viral and bacterial infections.

In mammals, the CXC chemokines have been reported to function in chemotaxis of neutrophils, monocytes and lymphocytes. However, the

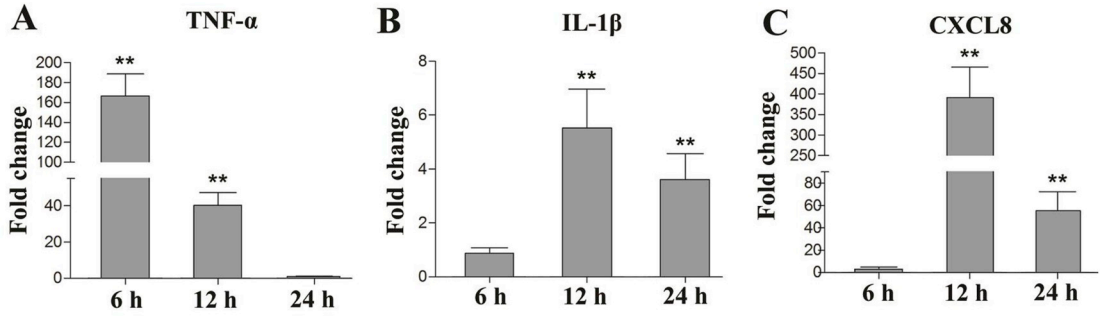

Fig. 7. Expression analysis of pro-inflammatory cytokines in PKMs treated with r*Lc*CXCL_F6.
Primary head kidney macrophages (PKMs) were treated with r*Lc*CXCL_F6 at a final concentration of 10 ng/mL, and harvested at different time points after treatment. PKMs were treated with the same concentration of rGST as controls. The relative expression levels of TNF-α (A), IL-1β (B), and CXCL8 (C) genes were normalized by β-actin and expressed as fold change compared with the controls (rGST-treated PKMs) at each time point. All data were obtained from three independent experiments with three replicates in each experiment. Error bars represent SEM of three independent experiments. $^{*}p < 0.05$; $^{**}p < 0.01$.

studies on chemotaxis and target cells of fish specific CXC chemokines are limited. The r*Lc*CXCL_F2 showed obvious chemotactic activity to monocytes/macrophages, lymphocytes and eosinophils [6]. Recombinant *Lc*CXCL8_L3 could attract the lymphocytes and eosinophils [21], and carp CXCb showed a strong chemotactic activity towards monocytes, granulocytes and lymphocytes [29]. In our study, r*Lc*CXCL_F6 showed obvious chemotactic activity to monocytes/macrophages and lymphocytes (Fig. 5). Mammalian CXC chemokines have been divided into two subgroups: ELR-positive subgroup and ELR-negative subgroup, based on the presence or absence of the ELR motif. The ELR motif is responsible for receptor binding and activation of neutrophils, and CXC chemokines that lack this motif act on monocytes and lymphocytes [30]. *Lc*CXCL_F6 lacks the ELR motif and its potential target cells are monocytes/macrophages and lymphocytes (Fig. 5 B), suggesting that *Lc*CXCL_F6 may possess a similar chemotactic activity to mammalian ELR-negative CXC chemokines. Production and release of NO have been considered as a clear indication for respiratory burst in macrophages and play an important role in the inflammatory response [31,32]. The production of NO in the body is catalyzed by inducible nitric oxide synthase (iNOS) [33]. In this study, we observed significant increases of NO production and iNOS expression in the r*Lc*CXCL_F6-treated PKMs (Fig. 6), implying that increased respiratory burst in the r*Lc*CXCL_F6-treated PKMs may result from iNOS induction. Pro-inflammatory cytokines (such as TNFα, IL-1β, IL-6, and IL-8) play key roles in mediating inflammatory response [34]. Most of these pro-inflammatory cytokines in teleost could be found their mammalian counterparts, and they exhibited conserved pro-inflammatory activities [35,36]. Therefore, we further tested the effect of r*Lc*CXCL_F6 on pro-inflammatory cytokine expression in PKMs and found that *Lc*CXCL_F6 could significantly up-regulate the expression levels of TNF-α, IL-1β, and CXCL8. These results support that *Lc*CXCL_F6 plays a role in mediating inflammatory response in large yellow croaker.

In conclusion, we identified a new member of fish specific CXC chemokines (*Lc*CXCL_F6) in large yellow croaker. *Lc*CXCL_F6 was constitutively expressed in all tested tissues and three immune-related cells, and was significantly up-regulated in the spleen and head kidney by poly (I:C) and *V. alginolyticus*. The r*Lc*CXCL_F6 not only exhibited chemotactic activity for lymphocytes and monocytes/macrophages from PBLs, but also enhanced the NO release and pro-inflammatory cytokine expression in PKMs, indicating that *Lc*CXCL_F6 plays a role in the inflammatory response.

Acknowledgements

The work was supported by grants from the National Natural Science Foundation of China (U1605211, 31772874, and 31802337), China Agriculture Research System (CARS-47), and Yantai Marine Economic Innovation and Development Demonstration City Industrial Chain Collaborative Innovation Project (YHCX-SW-L-201703).

Appendix A. Supplementary data

Supplementary data to this article can be found online at https://doi.org/10.1016/j.fsi.2018.10.068.

References

[1] C.E. Hughes, R.J.B. Nibbs, A guide to chemokines and their receptors, FEBS J. 285 (16) (2018) 2944–2971.
[2] M.P. Keane, D.A. Arenberg, B.B. Moore, C.L. Addison, R.M. Strieter, CXC chemokines and angiogenesis/angiostasis, Proc. Assoc. Am. Phys. 110 (4) (1998) 288–296.
[3] P. Bhatt, V. Kumaresan, R. Palanisamy, G. Ravichandran, K. Mala, S.M.N. Amin, A. Arshad, F.M. Yusoff, J. Arockiaraj, A mini review on immune role of chemokines and its receptors in snakehead murrel Channa striatus, Fish Shellfish Immunol. 72 (2018) 670–678.
[4] M.C. Miller, K.H. Mayo, Chemokines from a structural perspective, Int. J. Mol. Sci. 18 (10) (2017) E2088.
[5] E.J. Fernandez, E. Lolis, Structure, function, and inhibition of chemokines, Annu. Rev. Pharmacol. Toxicol. 42 (2002) 469–499.
[6] S. Zhou, Y. Mu, Y. Liu, J. Ao, X. Chen, Identification of a fish specific chemokine CXCL_F2 in large yellow croaker (*Larimichthys crocea*) reveals its primitive chemotactic function, Fish Shellfish Immunol. 59 (2016) 115–122.
[7] B. Gorgoglione, E. Zahran, N.G.H. Taylor, S.W. Feist, J. Zou, C.J. Secombes, Comparative study of CXC chemokines modulation in brown trout *(Salmo trutta)* following infection with a bacterial or viral pathogen, Mol. Immunol. 71 (2016) 64–77.
[8] T. Yoshimura, K. Matsushima, S. Tanaka, E.A. Robinson, E. Appella, J.J. Oppenheim, E.J. Leonard, Purification of a human monocyte-derived neutrophil chemotactic factor that has peptide sequence similarity to other host defense cytokines, Proc. Natl. Acad. Sci. U. S. A. 84 (24) (1987) 9233–9237.
[9] R.M. Strieter, P.J. Polverini, S.L. Kunkel, D.A. Arenberg, M.D. Burdick, J. Kasper, J. Dzuiba, J. Van Damme, A. Walz, D. Marriott, et al., The functional role of the ELR motif in CXC chemokine-mediated angiogenesis, J. Biol. Chem. 270 (45) (1995) 27348–27357.
[10] Q. Fu, Q. Zeng, Y. Li, Y. Yang, C. Li, S. Liu, T. Zhou, N. Li, J. Yao, C. Jiang, D. Li, Z. Liu, The chemokinome superfamily in channel catfish: I. CXC subfamily and their involvement in disease defense and hypoxia responses, Fish Shellfish Immunol. 60 (2017) 380–390.
[11] M. Oh, S. Bathige, Y. Kim, S. Lee, H. Yang, M.J. Kim, J. Lee, A CXCL ortholog from *Hippocampus abdominalis*: molecular features and functional delineation as a pro-inflammatory chemokine, Fish Shellfish Immunol. 67 (2017) 218–227.
[12] A.M. Cole, T. Ganz, A.M. Liese, M.D. Burdick, L. Liu, R.M. Strieter, Cutting edge: IFN-inducible ELR- CXC chemokines display defensin-like antimicrobial activity, J. Immunol. 167 (2) (2001) 623–627.
[13] A. Alejo, C. Tafalla, Chemokines in teleost fish species, Dev. Comp. Immunol. 35 (12) (2011) 1215–1222.
[14] J. Chen, Q. Xu, T. Wang, B. Collet, Y. Corripio-Miyar, S. Bird, P. Xie, P. Nie, C.J. Secombes, J. Zou, Phylogenetic analysis of vertebrate CXC chemokines reveals novel lineage specific groups in teleost fish, Dev. Comp. Immunol. 41 (2) (2013) 137–152.
[15] G.D. Wiens, G.W. Glenney, S.E. Lapatra, T.J. Welch, Identification of novel rainbow trout (*Onchorynchus mykiss*) chemokines, CXCd1 and CXCd2: mRNA expression after *Yersinia ruckeri* vaccination and challenge, Immunogenetics 58 (4) (2006) 308–323.
[16] J. Ao, Y. Mu, L.X. Xiang, D. Fan, M. Feng, S. Zhang, Q. Shi, L.Y. Zhu, T. Li, Y. Ding, L. Nie, Q. Li, W.R. Dong, L. Jiang, B. Sun, X. Zhang, M. Li, H.Q. Zhang, S. Xie, Y. Zhu, X. Jiang, X. Wang, P. Mu, W. Chen, Z. Yue, Z. Wang, J. Wang, J.Z. Shao,

X. Chen, Genome sequencing of the perciform fish *Larimichthys crocea* provides insights into molecular and genetic mechanisms of stress adaptation, PLoS Genet. 11 (4) (2015) e1005118.
[17] X. Wan, X. Chen, Molecular cloning and expression analysis of a CXC chemokine gene from large yellow croaker *Pseudosciaena crocea*, Vet. Immunol. Immunopathol. 127 (1–2) (2009) 156–161.
[18] C. Tian, Y. Chen, J. Ao, X. Chen, Molecular characterization and bioactivity of a CXCL13 chemokine in large yellow croaker *Pseudosciaena crocea*, Fish Shellfish Immunol. 28 (3) (2010) 445–452.
[19] C. Li, C.L. Yao, Molecular and expression characterizations of interleukin-8 gene in large yellow croaker (*Larimichthys crocea*), Fish Shellfish Immunol. 34 (3) (2013) 799–809.
[20] Y. Mu, K. Wang, J. Ao, X. Chen, Molecular characterization and biological effects of a CXCL8 homologue in large yellow croaker (*Larimichthys crocea*), Fish Shellfish Immunol. 44 (2) (2015) 462–470.
[21] S. Zhou, Y. Mu, J. Ao, X. Chen, Molecular characterization and functional activity of CXCL8_L3 in large yellow croaker *Larimichthys crocea*, Fish Shellfish Immunol. 75 (2018) 124–131.
[22] S. Yang, Q. Li, Y. Mu, J. Ao, X. Chen, Functional activities of interferon gamma in large yellow croaker *Larimichthys crocea*, Fish Shellfish Immunol. 70 (2017) 545–552.
[23] X.H. Wang, K.R. Wang, P. Nie, X.H. Chen, J.Q. Ao, Establishment and characterization of a head kidney cell line from large yellow croaker *Pseudosciaena crocea*, J. Fish. Biol. 84 (5) (2014) 1551–1561.
[24] I. Letunic, P. Bork, 20 years of the SMART protein domain annotation resource, Nucleic Acids Res. 46 (D1) (2018) D493–D496.
[25] H. Nielsen, Predicting secretory proteins with SignalP, Methods Mol. Biol. 1611 (2017) 59–73.
[26] K. Tamura, G. Stecher, D. Peterson, A. Filipski, S. Kumar, MEGA6: molecular evolutionary Genetics analysis version 6.0, Mol. Biol. Evol. 30 (12) (2013) 2725–2729.
[27] Q.W. Xie, H. Cho, Y. Kashiwabara, M. Baum, J.R. Weidner, K. Elliston, R. Mumford, C. Nathan, Carboxyl terminus of inducible nitric oxide synthase. Contribution to NADPH binding and enzymatic activity, J. Biol. Chem. 269 (45) (1994) 28500–28505.
[28] K.J. Laing, C.J. Secombes, Chemokines, Dev. Comp. Immunol. 28 (5) (2004) 443–460.
[29] L.M. van der Aa, M. Chadzinska, L.A. Golbach, C.M. Ribeiro, B.M. Lidy Verburg-van Kemenade, Pro-inflammatory functions of carp CXCL8-like and CXCb chemokines, Dev. Comp. Immunol. 36 (4) (2012) 741–750.
[30] S. Bird, C. Tafalla, Teleost chemokines and their receptors, Biology 4 (4) (2015) 756–784.
[31] R.B. Lorsbach, W.J. Murphy, C.J. Lowenstein, S.H. Snyder, S.W. Russell, Expression of the nitric oxide synthase gene in mouse macrophages activated for tumor cell killing. Molecular basis for the synergy between interferon-gamma and lipopolysaccharide, J. Biol. Chem. 268 (3) (1993) 1908–1913.
[32] K.E. Iles, H.J. Forman, Macrophage signaling and respiratory burst, Immunol. Res. 26 (1–3) (2002) 95–105.
[33] F. Aktan, iNOS-mediated nitric oxide production and its regulation, Life Sci. 75 (6) (2004) 639–653.
[34] H.M. Herath, D.A. Elvitigala, G.I. Godahewa, N. Umasuthan, I. Whang, J.K. Noh, J. Lee, Molecular characterization and comparative expression analysis of two teleostean pro-inflammatory cytokines, IL-1beta and IL-8, from *Sebastes schlegeli*, Gene 575 (2 Pt 3) (2016) 732–742.
[35] F. Chen, X.J. Lu, L. Nie, Y.J. Ning, J. Chen, Molecular characterization of a CC motif chemokine 19-like gene in ayu (*Plecoglossus altivelis*) and its role in leukocyte trafficking, Fish Shellfish Immunol. 72 (2018) 301–308.
[36] J. Garcia-Castillo, E. Chaves-Pozo, P. Olivares, P. Pelegrin, J. Meseguer, V. Mulero, The tumor necrosis factor alpha of the bony fish seabream exhibits the in vivo proinflammatory and proliferative activities of its mammalian counterparts, yet it functions in a species-specific manner, Cell. Mol. Life Sci. 61 (11) (2004) 1331–1340.